NASA CONTRACTOR REPORT

NASA CR-2032



# ANALYSIS OF FATIGUE CRACK PROPAGATION

*by H. W. Liu*

*Prepared by*
SYRACUSE UNIVERSITY
Syracuse, N.Y. 13210
*for Lewis Research Center*

NATIONAL AERONAUTICS AND SPACE ADMINISTRATION • WASHINGTON, D. C. • MAY 1972

| 1. Report No. | 2. Government Accession No. | 3. Recipient's Catalog No. |
|---|---|---|
| CR-2032 | | |

| 4. Title and Subtitle | 5. Report Date |
|---|---|
| ANALYSIS OF FATIGUE CRACK PROPAGATION | May 1972 |
| | 6. Performing Organization Code |

| 7. Author(s) | 8. Performing Organization Report No. |
|---|---|
| H. W. Liu | None |
| | 10. Work Unit No. |

| 9. Performing Organization Name and Address | 11. Contract or Grant No. |
|---|---|
| Syracuse University<br>Syracuse, New York 13210 | NGR 33-022-105 |
| | 13. Type of Report and Period Covered |
| 12. Sponsoring Agency Name and Address | Contractor Report |
| National Aeronautics and Space Administration<br>Washington, D. C. 20546 | 14. Sponsoring Agency Code |

15. Supplementary Notes

Project Manager, Marvin H. Hirschberg, Materials and Structures Division, NASA Lewis Research Center, Cleveland, Ohio

16. Abstract

The correlation between fatigue crack propagation and stress intensity factor is analyzed. When one measures fatigue crack propagation rate, a crack increment, $\Delta a$, and its corresponding increment in load cycles, $\Delta N$, are measured. Fatigue crack propagation must be caused by a shear and/or a normal separation mode. Both of these two processes are discrete if one looks at the atomic level. If the "average" deformation and fracture properties over the crack increments, $\Delta a$, can be considered as homogeneous, if the characteristic discrete lengths of these deformation and fracture processes are much smaller than the crack increment per cycle, $\delta a$, if the plastic zone size is small, and if a plate is thick enough to insure a plane strain case, $da/dN$ is proportional to $\Delta K^2$. Any deviation of empirical data from this relation must be caused by the fact that one or more of these conditions are not satisfied. The effects of plate thickness and material inhomogeneity are discussed in detail. A shear separation mode of fatigue crack propagation is described and is used to illustrate the effects of material inhomogeneity.

| 17. Key Words (Suggested by Author(s)) | 18. Distribution Statement |
|---|---|
| Fatigue crack propagation<br>Fracture mechanics<br>Crack propagation | Unclassified - unlimited |

| 19. Security Classif. (of this report) | 20. Security Classif. (of this page) | 21. No. of Pages | 22. Price* |
|---|---|---|---|
| Unclassified | Unclassified | 42 | $3.00 |

* For sale by the National Technical Information Service, Springfield, Virginia 22151

TABLE OF CONTENTS

# I. INTRODUCTION

In the past decade, a large amount of research has been done in the field of fatigue crack propagation (1-18). The concept of crack tip stress field has been used to analyze experimental data (6). The stress intensity factor range, $\Delta K$, characterizes crack tip cyclic deformation and fatigue crack propagation rate. Typical fatigue crack propagation data are shown in Figure (1a). The data can be divided into three regions. In the low $\Delta K$ region, region I, the slope of the curve is more than four. As $\Delta K$ decreases, $da/dN$ decreases rapidly. The data seems to indicate the existence of a limiting $\Delta K$ value for non-propagating crack. In the intermediate $\Delta K$ region, region II, the slope of the line is close to two. The slope of the line in the high $\Delta K$ region, region III, is equal to or higher than four. Additional region II data are shown in Figure (1b). The slopes of the lines in this figure are all close to two. Many theories have been proposed to explain the characteristics of fatigue crack propagation data. In this study, the application of $\Delta K$ to correlate fatigue crack propagation will be analyzed. Some idealized conditions will be assumed in order to derive a functional relationship between fatigue crack propagation rate and $\Delta K$. The deviations from the idealized assumptions will be examined and their effects on fatigue crack growth analyzed. This study is not a comprehensive survey on fatigue crack propagation. Only those results directly concerned with the application of $\Delta K$ to analyze fatigue crack propagation will be analyzed.

## II. A CRACK IN AN INFINITE PLATE UNDER A CYCLIC LOAD

When a cracked plate is loaded, the material near a crack tip undergoes plastic deformation. For a small through crack in an infinite plate, if the plate thickness does not affect the stresses and strains, the crack length, 2a, is the only characteristic length of the plate. The dimensional analysis in the Appendix indicates that the stresses and strains at geometrically similar points, i.e. at homologous points in geometrically similar solids, are identical, if the solids are made of the same material with the same stresses at homologous points on the boundaries. The displacements at homologous points in these solids are linearly proportional to a. In other words, if the geometrically similar solids are scaled by their only characteristic length, a, after scaling, the stresses and strains at the same point of each of these solids are identical.

When a very large plate with a through crack is cyclically loaded, the material ahead of a crack tip undergoes repeated plastic deformation. When a material element is very close to a crack tip, the cyclic plastic strain range experienced by the material element is high and the cyclic deformation causes damage. If a material element is far away from a crack tip, the cyclic plastic strain range is low, and the damage incurred to the material element may be negligible.

In this section, a centrally cracked infinite plate with a constant cyclic applied stress range, $\Delta\sigma$ and a constant stress ratio, $R = \sigma_{min}/\sigma_{max}$, will be analyzed. Let $\delta a$ be a crack increment per cycle. If $\delta a$ is proportional to a, according to the dimensional analysis, the stresses and strains experienced by the material element within $\delta a$ must be the same regardless of the length of the crack. If one assumes that the deformation and fracture properties are homogeneous and that the stresses and strains experienced by the material element cause crack propagation, one cannot but conclude that

$$da/dN = C_1 a \tag{1a}$$

where $C_1$ is a proportional constant. To include the effects of stress ratio, one may write

$$da/dN = f_1(R)\, a \tag{1b}$$

where $f_1$ is a function of R. For a given value of R, $f_1$ is a constant.

If a material element is far away from a crack tip, the stresses and strains are low, and the material element is not damaged by the cyclic stresses and strains. When a material element enters the highly strained region close to a crack tip, the cyclic strains cause damage. According to the dimensional analysis, the size of the highly strained region must be

proportional to a. At various stages of crack propagation, the stress and strain cycles experienced by the material elements along the crack path must be the same, if the values of (r/a) at these points are the same, and if the crack propagates according to Equation (1). r is distance from the crack tip. If $\delta a$ is proportional to a, the stress and strain cycles experienced by the material element in $\delta a$ must be identical regardless of the crack length. In this case, Equation (1) is valid, even if the past stress and strain cycles experienced by a material element prior to its arrival at the crack tip affect crack growth. This problem was first analyzed by Dugdale et al. using an elastic model (2), and it was subsequently extended by Liu to elasto-plastic solids (3).

Since the materials at homologous points experience the same stresses and strains, the size of the plastic zone, $r_p$, must be proportional to a. Therefore, Equation (1) can also be written as

$$da/dN = C_2 \, r_p \tag{2a}$$

or

$$da/dN = f_2(R) \, r_p \tag{2b}$$

where $C_2$ is a proportional constant, and $f_2$ is a function of R.

In the derivations of Equations (1 and 2), two assumptions were made: namely the crack length is the only characteristic length and the material is homogeneous. The former condition is satisfied if the cracked plate is thick enough so that the plane strain condition prevails. When a plate is thin, necking occurs, and necking is strongly affected by plate thickness. In this case, both crack length and plate thickness are important length parameters that affect plastic deformation. The crack length alone cannot be used to scale the geometry of a cracked plate. In other words, even when $\delta a$ is proportional to a, the stresses and strains within $\delta a$ do not remain the same, as the crack propagates. Therefore, Equations (1 and 2) are no longer valid. The effects of plate thickness will be discussed in more detail in Section IV.

In the derivations of Equations (1 and 2) we have assumed the homogeneity of the deformation and fracture properties of the material elements along the crack path. In other words, if the material elements have experienced identical stress and strain cycles, these elements will have the same response to the same load during the next cycle. If the material elements are not homogeneous, the deformations within the $\delta a$'s at various stages of crack propagation may not be the same, even if the $\delta a$'s are proportional to their respective crack lengths. Even if the deformation within $\delta a$'s are the same, the fracture properties of these elements may differ, if

these elements are not homogeneous. The condition of material homogeneity assures that each crack increment, $\delta a$, is proportional to a. When one measures fatigue crack propagation rate, a crack increment of certain measurable length, $\Delta a$, and its corresponding increment in load cycles, $\Delta N$, are measured. For the practical applications of Equations (1 and 2), only the average deformation and fracture properties over the crack increment, $\Delta a$, need to be homogeneous, provided that the characteristic lengths of the discrete deformation and fracture processes are much smaller than $\delta a$, so that these processes can be treated as continuous. In the following discussions, the conditions of homogeneous average properties and the continuous deformation and fracture processes over $\delta a$ will be called the conditions of material homogeneity. These conditions will be discussed in detail in Sections V and VI.

According to the dimensional analysis in the Appendix, the stresses and strains at homologous points in geometrically similar solids are identical, if the boundary stresses are identical at geometrically similar regions on the boundaries. Two opposite line wedge forces, F, acting at the mid-points of the crack surfaces are shown in Figure (2). A line force F, can be considered as the total force given by a stress acting on a very narrow strip.

$$F = \lim_{\Delta W \to 0} \sigma \, \Delta W \tag{3}$$

where $\Delta W$ is the width of the narrow strip. If crack length, a, is the only length parameter, the width, $\Delta W$, must be linearly proportional to a, in order to maintain the condition that the boundary stresses are the same at homologous points. Therefore, in order to maintain the condition that gives rise to identical stresses and strains at homologous points, the line force F must increase linearly with a. Therefore da/dN is proportional to a, if F is kept proportional to a.

In the Appendix, the stress intensity factor of a cracked infinite plate with two opposite wedge forces acting at the mid-points of the crack surfaces is shown as

$$K = C_3 \frac{F}{\sqrt{a}} \tag{4}$$

where $C_3$ is a proportional constant. If the applied line forces are proportional to a, the stress intensity factor is proportional to $\sqrt{a}$. In this case, if da/dN is proportional to the square of the stress intensity factor range, $\Delta K^2$, it must be proportional to a. Consequently, dimensional analysis is applicable to the case of concentrated line force if appropriate dimensionless parameters are chosen. If Equations (1 and 2) do not agree with the experimental data, it is not because dimensional analysis is not applicable to fatigue crack growth as claimed earlier (7). Rather, the discrepancy is caused by the fact that one or more of the assumptions in the derivations of Equations (1 and 2) are not satisfied.

Following the same analysis, Equations (1 and 2) can be shown applicable to a penny shaped crack in an infinite solid under a uniform cyclic tensile stress. For two opposite point forces, F, applied at the centers of the circular crack surfaces, da/dN is proportional to a, if F is kept proportional to $a^2$.

## III. FATIGUE CRACK PROPAGATION RATE AND STRESS INTENSITY FACTOR RANGE

The application of stress intensity factor range to the analysis of fatigue crack propagation rate is one of the most important contributions to the study of fatigue in recent years (6,7). An overwhelming amount of data and numerous models on the correlation of da/dN with $\Delta K$ exist. A general survey was made by Paris and Johnson (18). This section presents a deductive analysis, which helps to interpret experimental data and aids in evaluating various models of fatigue crack propagation.

The elastic stresses in a cracked plate can be expressed in terms of infinite series (19). Close to a crack tip, the elastic stresses can be approximated by (19,20)

$$\sigma_{xx} = \frac{K}{\sqrt{2\pi r}} \cos(\theta/2)\,[1 - \sin(\theta/2)\sin(3\theta/2)]$$

$$\sigma_{yy} = \frac{K}{\sqrt{2\pi r}} \cos(\theta/2)\,[1 + \sin(\theta/2)\sin(3\theta/2)] \qquad (5)$$

$$\sigma_{xy} = \frac{K}{\sqrt{2\pi r}} \cos(\theta/2)\sin(\theta/2)\sin(3\theta/2)$$

$$\sigma_{zz} = 0 \qquad \text{for plane stress case}$$

$$\sigma_{zz} = \nu(\sigma_{xx} + \sigma_{yy}) \qquad \text{for plane strain case}$$

where r and $\theta$ are polar coordinates, with the crack tip as the origin and the crack lying along the line $\theta = \pi$, which coincides with the negative x-axis. Equations (5) give good approximations of the elastic stresses, only if the distance from the crack tip, r, is small enough. Let $r_e$ be the size of a small region near a crack tip within which Equations (5) are valid. If a material is elasto-plastic, the high stresses near a crack tip cause plastic deformation. Therefore, a small region of plastic deformation, $r_p$, exists at the crack tip. Both $r_e$ and $r_p$ are shown schematically in Figure (3). When plastic deformation occurs within $r_p$, the stresses in the vicinity of the crack tip are relaxed. Because of the stress relaxation, the actual stresses on $r_p$ differ from the calculated elastic stresses by an amount $\delta\sigma$. $\delta\sigma$ varies along $r_p$. It must be statically in equilibrium by itself. Therefore, its resultant force and resultant moment must be zero. According to Saint Venant's principle the change of the stresses on $r_e$ caused by the stress relaxation $\delta\sigma$, must be negligible, if $r_e >> r_p$. If the relaxation of the stresses on $r_e$ is negligible, the stresses on $r_e$ are essentially

those given by Equations (5), and the value of K is sufficient to characterize the stresses and strains within $r_p$, even if plastic deformation takes place. The condition, $r_e >> r_p$ can be realized either if $r_e$ is very large or if $r_p$ is very small. $r_e$ increases with specimen size and crack length. $r_p$ is small if the yield strength of a material is high and the applied stress is low.

When a cyclic load is applied, the cyclic stresses and cyclic strains within $r_p$ must be prescribed by the stress intensity factor range, $\Delta K$, and the stress ratio R. The high strain gradient near a crack tip induces $\sigma_{zz}$ $\sigma_{xz}$ and $\sigma_{yz}$ and their corresponding strain components. These stresses and strains and their effects on other crack tip stress and strain components are strongly affected by plate thickness. Crack tip deformation has been measured. The results of these measurements clearly indicate that crack tip deformation is affected by $\Delta K$, R, and plate thickness (21). If fatigue crack propagation is caused by the stresses and strains experienced by the material element at the crack tip, one concludes that da/dN is a function of $\Delta K$, R, and plate thickness, i.e.

$$da/dN = f_3 (\Delta K, R, \text{thickness}) \qquad (6)$$

If a plate is thick enough, so that the state of plane strain prevails, Equation (6) can be written as

$$da/dN = f_4 (\Delta K, R) \qquad (7)$$

The functional relation between da/dN and $\Delta K$, R, and plate thickness can be found empirically. The thickness effect on da/dN has been observed (10).

The above conclusion is not subject to the limitations of "material homogeneity". It is valid even if the crack propagation mechanism is a discrete process. Equations (6 and 7) were deduced from the simple assumption that, with the same applied cyclic stresses on $r_e$, the same events must happen and da/dN must be the same. But it does not establish any functional relation between da/dN and $\Delta K$.

Next we want to deduce a specific relation between da/dN and $\Delta K$ for a thick plate and for a material which is "homogeneous" in its deformation and fracture properties. Let us examine the stresses and strains near the crack tips in plates loaded to various $\Delta K$ values. The specimens are thick

enough so that the condition of plane strain prevails. Assume that the value of R is the same for all the specimens. If the condition of $r_e >> r_p$ is satisfied in all cases and if we let $r_e$ be proportional to $(\Delta K)^2$, the stresses at the homologous points on the boundaries of $r_e$'s must be the same. If we look at $r_e$ as isolated from the rest of a specimen, $r_e$ is the only length parameter of the region of interest to us. Therefore, the regions near the crack tips can be scaled by their respective $r_e$'s. The dimensional analysis in the Appendix concludes that the stresses and strains at the homologous points within $r_e$'s must be identical. Consequently $r_p$ must be proportional to $r_e$. Under a cyclic load, $r_p$ for cyclic plastic deformation must be proportional to $\Delta K^2$, and it must be related to the cyclic yield strength of a material. If each crack increment is proportional to its $r_p$, the cyclic stresses and strains within every increment must be identical. If the condition of material homogeneity is satisfied, one cannot but conclude:

$$da/dN = f_5 (R)\, r_p \tag{8a}$$

or

$$da/DN = f_6 (R)\, \Delta K^2 \tag{8b}$$

Equation (8b) has been shown applicable to thick plates made of nineteen materials (11,22). Some of the data are shown in Figure (1b).

The conditions that lead to Equations (8a and 8b) are $r_e >> r_p$, plane strain state of stresses and strains, and material homogeneity. This first condition is satisfied if $r_p$ is much smaller than the crack length and the ligament size of a specimen or if the applied stresses are much lower than the yield strength of a material. Both thickness effect and material homogeneity will be discussed in subsequent sections.

## IV. THICKNESS EFFECTS ON CRACK TIP DEFORMATION AND FATIGUE CRACK PROPAGATION

The conclusion that da/dN is proportional to a or $r_p$ is valid, if a two-dimensional analysis is applicable to a cracked plate, so that a or $r_p$ is the only relevant length parameter. Both plane stress and plane strain analyses are frequently used for two-dimensional plate problems. If a plate is very thick, plane strain analysis is applicable; and if a plate is very thin, plane stress analysis is often used. In either model, one assumes that the stresses and strains are independent of plate thickness. If plate thickness affects the stresses and strains, a single length parameter such as a or $r_p$ is not sufficient to characterize the state of stresses and strains near a crack tip. The thickness parameter has to be taken into consideration. In this case, Equations (1,2,7, and 8) are no longer valid.

The plane strain and plane stress analyses are idealized models. The stresses and strains near a crack tip in a plate are much more complicated. The high stresses near a crack tip cause plastic deformation. The plastic strains $\varepsilon^p_{xx}$ and $\varepsilon^p_{yy}$ are very high near a crack tip. The condition of volume constancy requires that $\varepsilon^p_{zz} = -(\varepsilon^p_{xx} + \varepsilon^p_{yy}).\varepsilon^p_{zz}$ is the contraction of the plate thickness. A high strain gradient exists near a crack tip. A region closer to a crack tip has higher strains and tends to contract more. But the region is constrained from contraction by the region of lower strains farther out. This constraint resists thickness contraction and induces the tensile stress, $\sigma_{zz}$, and the elastic tensile strain, $\varepsilon^e_{zz}$ in the direction of the plate thickness. In the interior of a very thick plate, the displacement in the thickness direction is negligibly small, and the deformation approaches that of plane strain. On the plate surface, stresses must be zero, therefore the conditions of plane stress prevail. For a thick plate, the state of stresses and strains changes gradually from that of plane stress on the surface to that of plane strain in the interior. This is true if the plastic zone size is small relative to the plate thickness. It is also clear that the rate of transition from the state of plane stress on the surface to the state of plane strain in the interior depends on strain gradient. If the gradient is high, the transition is fast, and if the gradient is low, the transition is slow. If there is no strain gradient in the plane of a plate, tensile stress in the plate thickness direction cannot be induced, regardless of how thick the plate is. Close to a crack tip, the strain gradient is steep and the rate of transition is fast. At a short distance away from the plate surface the transition to the state of plane strain is completed. As r increases, the strain gradient decreases, and the thickness of the transition layer increases. Far away from a crack tip, the state of stresses and strains throughout the plate thickness is essentially that of plane stress.

A schematic picture of the plane strain plastic zone in a thick plate near a crack tip is shown in Figure (4). The size of the plane strain zone starts from zero on the plate surface and grows to the fully developed size in the interior, if a plate is thick enough. In the interior of a thick plate, the plane strain plastic zone, $r_{p\varepsilon}$, coincides with $r_p$. Close to the plate surface $r_p$ becomes bigger, but $r_{p\varepsilon}$ becomes smaller. The length of the fully developed plane strain region, $\eta$, relative to the size of the transition region, depends on the size of the plastic zone relative to the plate thickness. $\eta$ is longer for a thicker plate and a smaller $r_p$. Within the plane strain region, the maximum tensile stress is much higher than that in the transition region. It should be pointed out that even if the conditions of plane strain are satisfied within $r_{p\varepsilon}$ in the transition layer, the stresses and strains at a given distance r are not the same as those in the interior of the specimen. This is obvious because the stresses just outside of $r_{p\varepsilon}$ are not the same in these two different regions. However, this difference decreases with r. At a short distance from a crack tip in a very thick plate the stresses and strains along the entire crack front, except two small regions near both ends, agree with that of a plane strain case. If the stress and strain cycle at a crack front controls the rate of crack propagation, and if the condition of plane strain together with others are met, Equations (1, 2, 7, and 8) are valid and applicable to thick plates.

In the transition layer, $r_p$ is larger than $r_{p\varepsilon}$. A material element reaches $r_p$ first,then it enters $r_{p\varepsilon}$. The material in the transition layer experiences more cycles of plastic strain and the amplitudes of the strain cycles are higher than those in the plane strain region. If the cyclic plastic deformation alone causes damage and crack propagation, da/dN in the transition layer should be faster. On the other hand, the maximum tensile stress in the plane strain region is much higher, therefore the material there can sustain much less total cyclic plastic strain. This high tensile stress in the plane strain region increases crack propagation rate. Apparently, the high tensile stress in the plane strain region has a more dominant effect on crack propagation rate. Consequently, the center portion of a crack front propagates faster and it leads the two ends as shown schemcatically in Figure (5). $\beta$ is the difference in the crack lengths in the specimen interior and the specimen surface. The curvature of the crack front in the transition region causes an increase in the strain from that of a straight crack front. This increase in strain increases da/dN in the transition region, so that the lag, $\beta$, of the surface crack is reduced. If the lag is small in comparison with the overall crack length, a, the measured crack propagation rate is essentially that in the interior of a specimen. If $\beta$ is linearly proportional to $\Delta K^2$, the measured da/dN differs from the rate in the interior by a small constant factor. In either case, a plane strain analysis is applicable to fatigue crack propagation, and Equations (1, 2, 7, and 8)

are valid for a thick plate. Clark and Trout (11) tested Ni-Mo-V alloy steel at both 75°F and 0°F. As the specimen thickness increases from 1 inch to 2 inches, the experimental data conform to Equation (8b).

When a plate is thin, plane stress analysis is often used. When strain is not excessive, a two-dimensional plane stress model can be a very good approximation. When strain exceeds certain limit, local necking takes place, and the stresses and strains are functions of plate thickness and the coordinate Z, which is normal to the plate. Consequently, a or $r_p$ alone is not sufficient to characterize the stresses and strains within the highly strained region ahead of a crack tip. The assumption of geometric similitude is no longer met, and the validity of Equations (1, 2, 7, and 8) has to be examined. Both steep strain gradient and excessive local strain concentration ahead of a crack tip enhance necking. Figure (6) shows a schematic diagram of a necked region imbedded in a plastic zone.

After necking takes place, the materials above and below the narrow strip deform very little. The opening displacement, v, and the length of the strip necking region were calculated by Dugdale (23), Goodier and Fields (24), Bilby, Cottrell, and Swinden (25) and Rice (26). In these calculations, the overall crack length was assumed to be the sum of the length of the real crack and the length of the strip necking region. On the surfaces of the real crack, the stresses are zero. On the upper and the lower boundaries of the strip necking region, a tensile stress equal to the yield strength of the material, $\sigma_Y$, is applied. Effectively, the model assumes an elastic and perfectly plastic solid. Plastic deformation is restricted to the strip necking zone, and the rest of the plate is elastic. The opening displacement v is given by

$$v(x,a) = \frac{\sigma_Y \ell}{\pi E}\left[\cos\theta \log \frac{\sin^2(\theta_2 - \theta)}{\sin^2(\theta_2 + \theta)} + \cos\theta_2 \log \frac{(\sin\theta_2 + \sin\theta)^2}{(\sin\theta_2 - \sin\theta)^2}\right] \tag{9a}$$

where

$$\cos\theta_2 = a/\ell \tag{9b}$$

$$\cos\theta = x/\ell \text{ for } |x| < \ell, \text{ and } -\pi < \theta < \pi \tag{9c}$$

$$\theta_2 = \pi\sigma/2\sigma_Y \tag{9d}$$

and a is the half crack length, and $\ell$ is the sum of a and the length of the strip necking zone, $r_p$. For small scale yielding

$$r_p = \pi K^2/8\sigma_Y^2 \tag{10}$$

At the crack tip, the relative opening displacement between the upper and the lower crack surfaces is

$$\delta_o = K_I^2/E\sigma_Y \tag{11}$$

The opening displacements in a thin steel sheet were measured using moire method (27). Figure (7) shows the picture of the moire pattern of a slotted thin steel sheet under a tensile load. The steel sheet is 0.012 inches thick and 6 inches wide. The slot is a one inch long jeweler's saw cut 0.007 inches wide. The region of strip necking at the end of the thin slot is clearly visible. Both the calculated and measured opening displacements are plotted in Figure (8). The measured and the calculated values at each end of the slot show good agreement.

When necking takes place, shear deformation occurs on two mutually orthogonal planes. Both planes are inclined at 45° to the axis of the tensile load and to the plane of the plate. As slip takes place on these two planes, the sheet thickness is reduced. Figure (9) is a schematic diagram showing the opening displacements v, and the thickness contraction w. The thickness contraction in the strip necking region was measured with a microscope. The microscope was first focussed on the specimen surface, then on the bottom of the necking region. The reduction of the specimen thickness is the difference of the readings on the micrometer, which is attached to the microscope for focus adjustment. Because of the shallow depth of focussing at high magnifications, the thickness contraction can be measured accurately. Both opening displacement and thickness contraction were measured after the specimen was unloaded. The measurements are shown in Figure (10). The values of the thickness contractions and opening displacements agree very well with each other.

The average contraction strain in the thickness direction, $\varepsilon_{zz}$ within the strip necking region is given by

$$\varepsilon_{zz} = 2w/t = -2v/t$$

where t is plate thickness. Assuming volume constancy and that $\varepsilon_{xx}$ is negligible, together with the relation between K and v (26), we obtain

$$\varepsilon_{yy} = (K^2/Et\sigma_Y)\left\{(1-x/r_p)^{1/2} - \frac{1}{2}\frac{x}{r_p}\log\left[\frac{1+(1-x/r_p)^{1/2}}{1-(1-x/r_p)^{1/2}}\right]\right\} \tag{13}$$

for small scale yielding, where $r_p$ is the length of the strip necking zone given by Equation (10).

Therefore both the length of a strip necking region and the strain in the region are proportional to $K^2$. The necking model gives a strain which is inversely proportional to t. The strain measurements made in the area close to the strip necking zone indicate that plastic deformation spreads outside of the necking zone. A more detailed discussion on the strain measurements in the strip necking region was given in an earlier paper (27).

For small scale yielding in an elasto-plastic plate without necking, the $\varepsilon_{yy}$ is linearly proportional to K. When necking takes place $\varepsilon_{yy}$ is proportional to $K^2$. As a crack propagates, K and $r_p$ increase. When $r_p$ is sufficiently large, necking takes place, and the rates of increases in $r_p$ and the strains in the necking region become faster than those given by a two-dimensional plane stress model. If crack growth is caused by cyclic deformation, da/dN should increase with a much faster rate after necking takes place. If da/dN is expressed in terms of $\Delta K^n$, n should be larger than 2, and Equations (1, 2, 7 and 8) are no longer applicable. Liu (3) has suggested earlier that a plane stress model is applicable to analyze fatigue crack growth in thin plates. The above analysis and the empirical results clearly indicate the contrary. Therefore we may conclude that Equations (1, 2, 7 and 8) are applicable only to thick plates when $r_p$ is small.

## V. THE EFFECTS OF MATERIAL HOMOGENEITY

In the derivations of Equations (1, 2, and 8) the deformation and fracture properties of a material were assumed to be homogeneous. The material homogeneity does not mean that the stress strain characteristics are the same throughout a specimen at any instant. It rather means that the material will exhibit the same stress-strain characteristics, after experiencing the same stress-strain history. The material near a crack tip having experienced a number of high strain cycles will exhibit different stress-strain characteristics from the material far away from a crack.

Real materials always contain various types of inhomogeneity such as point defects, dislocations, different phases of an alloy, grain boundaries, etc. The processes of plastic deformation and fracture are inherently inhomogeneous due to the fact that materials are discrete in nature rather than continuous. Only the average properties over a large enough volume can be considered as homogeneous.

The generation and the movement of dislocations cause plastic deformation. Figure (11) shows a glide lamella and slip steps caused by plastic deformation of a single crystal. Extensive plastic deformation is concentrated in slip bands separated by undeformed lamella. The thickness of an undeformed packet in an aluminum single crystal is about 200 Å and the height of the slip steps is about 2000Å (28). When a crystal is not optimumly oriented for single slip, several slip systems will be activated simultaneously. Multiple slips within a band have often been observed (29). The spacings between slip bands decrease as strain increases.

When a single crystal is cyclically deformed, subgrains are formed (30). The size of the subgrain decreases as the cyclic strain amplitude increases. A subgrain boundary consists of numerous dislocations. These dislocations in a subgrain boundary must be generated by cyclic plastic deformation. All of these studies indicate the inhomogeneous nature of plastic deformation, i.e. extensive plastic deformation concentrates on certain planes which are separated by regions of little or no plastic deformation. Only the average plastic deformation over a large enough volume can be considered as homogeneous.

Plastic deformation can cause the formation of microcracks. Stokes and Li (31) have found that microcracks in sodium chloride extend to form slits along channels between slip bands. This is because a slip band resists crack propagation across them but it enhances propagation parallel to them. They found that local plastic constraint is the main factor responsible for extending a surface microcrack. Parker (32) has observed that a crack was nucleated in a MgO single crystal from the shears on two intersecting slip bands. Cracking has been observed at a kink plane in zinc (33). The crack is caused by the splitting in two of a tilt boundary at the kink plane.

Furthermore, the stresses and strains at the tip of a pile-up of dislocations are equivalent to those of a crack (34,35). Stokes has shown that a crack can be nucleated by a dislocation pile-up at a barrier (36). Hahn et al. (37) have shown that local heterogeneous deformations, slip bands or twins, may provide constraint and cause cracking in polycrystal iron and steel. Ryder and Smale (38) have shown that transcrystalline fractures of an aluminum alloy containing 7.3% zinc and 2.6% magnesium are caused by the formation of lens-shaped voids. These voids cause shallow depressions on a fracture surface. At the center of a depression, a particle of compound often exists.

It has been shown by photomicrographs that fatigue fracture is initiated at localized slip markings (39,40). As the number of cycles of load increases, a slip marking develops into a surface crack. In 2024-T4 aluminum alloy, it has been found that concentrated slip occurs around inclusions (41). Cracks are eventually nucleated in the area of severe but localized slip. The fractograph in Figure (12) shows the fracture surface of a cyclically loaded specimen. The striations and the particle indicate the inhomogeneous fracture properties of the material elements on the fracture surface.

All of these studies indicate that fracture is a discrete process. The fracture characteristics vary from one point to another in a solid. Only the average fracture property, over a large enough volume to take care of the statistical variation, is homogeneous. When one measures crack propagation rate, a crack increment, $\Delta a$, and its corresponding increment in load cycles, $\Delta N$, are measured. Only the average properties of the increment $\Delta a$ have to be homogeneous.

When the characteristic length parameters of a particular kind of material inhomogeneity are much smaller than a crack increment, $\delta a$, the average properties of the material over $\delta a$ can be considered as homogeneous. For example, if the size and the spacing of microcracks, which are generated by the cyclic plastic deformation, are much smaller than $\delta a$, the average effects of these microcracks on the deformation and fracture properties over the area $\delta a$ can be considered as homogeneous. Therefore, the assumption of material homogeneity is satisfied.

Commercial structural materials often contain regions of low fracture strength such as the brittle particle in Figure (12). Often the percentage of these low strength regions is low. When $\Delta K$ is low, the spacing between the particles is much larger than $\delta a$, and the path of the fatigue crack is not disturbed by the particles. In this case, the effects of these particles on fatigue crack propagation is negligible, and the material can be considered as "homogeneous".

On the other hand, the coherent precipitation particles in an aluminum alloy are very small. At the optimum strength level its size is only a small

fraction of a micro-inch. The strength of these particles could be either stronger or weaker than the matrix. If a crack increment is several micro-inches wide and each crack increment contains numerous particles, the material can be considered as homogeneous.

Fatigue crack propagation can be normal separation mode or shear separation mode. Microcracks, brittle particles, and triaxial state of stress enhance the normal separation mode. The ductility of a material in general and the lack of microcracks, brittle particles and triaxial state of stress enhance shear separation mode.

If $r_e >> r_p$, if the plane strain condition prevails, and if the material can be considered as homogeneous, at various stages of crack propagation, the region ahead of a crack tip can be scaled by $r_p$ so that at geometrically similar points the past stress and strain histories together with the present deformation and fracture properties are the same. Therefore the extent of crack growth by either normal or shear separation mode must be proportional to the characteristic length $r_p$. When the characteristic length of a discrete deformation or fracture process, which is essential to the mechanism of fatigue crack propagation, is comparable to $\delta a$, the material can no longer be treated as homogeneous, and the characteristic length has to be included in an analysis. In the following section, a shear separation mode of fatigue crack propagation will be illustrated and the effect of the characteristic length of the discrete shear deformation process on fatigue crack growth will be illustrated.

## VI. FATIGUE CRACK PROPAGATION - A MODEL OF SHEAR SEPARATION MODE

A crack can grow in a shear separation mode caused by slips on two sets of orthogonal shear planes. Figure (13a) shows a crack tip and its immediate vicinity. On the plane of the crack, there is no shear stress, therefore the shear planes for the state of plane strain deformation must be inclined 45° to the plane of the crack as shown in the figure. As discussed earlier, shear deformation is not a homogeneous process. It concentrates on certain slip planes, separated by regions of low or no deformation. Let us assume that the shear lines in Figure (13a) are the shear planes. At first, the shear line "α" is activated. The upper left hand side of the solid moves in the direction of the shear line until the tip of the upper crack surface reaches the shear line "b" as shown in Figure (13b). In this process, a new segment of the crack surface is created along the shear line α. As the load is further increased, the shear line "b" is activated, the lower left hand side of the solid moves in the direction of the line "b". After the shear movements on slip planes α and b, the new crack configuration is shown in Figure (13c).

This process can be repeated successively along shear lines, β and c. After the shear deformations on the second set of shear planes, the crack tip is advanced to a new position as shown in Figure (13d). After a great number of shear lines are activated during the loading cycle, the crack profile at the maximum load is given in Figure (13e).

When the specimen is unloaded the shear deformations along the shear lines will be reversed. However the reversed shear deformation will be less than the forward shear motion. Therefore the newly formed crack surfaces will not grow backwards. This is obvious if one considers a slip band as a shear crack with internal frictional shear stress acting on the crack surfaces. An elastic crack is shown in Figure (14a). When the specimen is loaded, a shear step is formed as shown in Figure (14b). If there is no frictional shear stress on the crack surfaces, upon unloading, the shear step will disappear and the specimen is reverted to its original shape as shown in Figure (14a). If a frictional shear stress exists between the crack surfaces, upon unloading, the shear step will be reduced but it does not disappear entirely as shown in Figure (14c). The slip bands are equivalent to shear cracks with frictional shear stress between crack surfaces. Closer to the new crack tip, the percent of the shear deformation recovered during the unloading cycle would be higher. Therefore upon unloading, the crack profile is given in Figure (13f).

In the process of the shear separation mode of crack growth, the plastic deformation is not limited to a narrow strip such as suggested by Dugdale model (23). Therefore the opening displacement at a crack tip will be much less than that given by the Dugdale model. Nevertheless if the area ahead

of the crack tip can be scaled by $r_p$ so that as a crack propagates the condition of geometric similitude is maintained, the crack tip opening displacement is proportional to $r_p$ and $\Delta K^2$. Therefore da/dN is proportional to $\Delta K^2$.

When the spacings between the neighboring activated shear lines are much smaller than the crack increment $\delta a$, the deformation can be considered as "continuous" and the average deformation property over $\delta a$ is homogeneous. In this case, Equations (1, 2, and 8) are valid.

The region II data in Figure (1) substantiates the validity of Equation (8b). In region I of the figure, Equation (8b) is not valid, but Equation (6) or (7) is applicable. In this region, both $\Delta K$ and da/dN are low. The slope of the curve in this region is often equal to or more than 4. The transition from region I to region II often takes place in the da/dN range of 1 to 5 μ in/cycle. This transition point is approximately equal to the thickness of the undeformed packet as shown in Figure (11). This thickness could be the separation of the neighboring shear lines of the shear separation mode of fatigue crack propagation as shown in Figure (13). If the crack growth rate is less than the separation between neighboring shear lines, the shear step on the shear line α in Figure (13a) does not reach the shear line b. Upon unloading, the length of the shear step will be reduced by the reversed shear flow. Thus, the crack growth rate is much less. This may account for the sharp drop in da/dN as $\Delta K$ is reduced to below the transition point. Therefore in region I, the discrete nature of shear deformation has to be taken into consideration, and the material cannot be considered as homogeneous. Consequently the assumption of material homogeneity in the derivations of Equations (1, 2, and 8) is no longer valid, and the experimental data indicate that the equations are not applicable in region I.

Commercial structural metals are polycrystals. The grain orientation varies from one to the next. Because of the complicated multiaxial crack tip stress field, it is most likely that several slip systems are activated. The macroscopic plastic deformation is the result of dislocation movements on these slip systems, and the anisotropic effects of grain orientation are "smoothed" out. For an isotropic solid, the slip lines are inclined 45° to the plane of the crack. The anisotropic deformation property of a crystal changes the angle of inclination. We have discussed shear and normal separation modes separately, but fatigue crack propagation is most likely the result of the combination of both.

## VII. DISCUSSIONS

Fatigue crack propagation can be analyzed in terms of energies or plastic deformation. Paris (8) and Roney (17) relate fatigue crack propagation rate to plastic deformation energy near a crack tip. Energy criterion has been widely used to analyze physical phenomena. Often two energy quantities are involved in such analyses. For example, the elastic energy released by a cracked solid and the energy of the newly formed crack surfaces were used by Griffith to analyze brittle fractures. Such an analysis involving two energy quantities gives a good insight into the physical problem.

The alternative to an energy analysis is to study the effects of crack tip deformation on fatigue crack propagation. Both crack tip opening displacement and near tip strain have been used to analyze fatigue crack growth. The experimental data on crack tip deformation strongly suggest that the Dugdale model is applicable only to the case of crack tip necking. Necking takes place only when a plate is thin and the plastic zone is large enough to cause slips on two mutually perpendicular shear planes as shown in Figure (9). Therefore Dugdale model is not applicable to calculate the crack tip opening displacement in a plane strain case in a thick plate. However, a simple dimensional analysis indicates that the crack tip opening displacement is proportional to $\Delta K^2$ for small scale yielding.

Two major objectives of fatigue crack propagation investigations are to collect data for engineering designs and safety inspections and to analyze the material property with the purpose of improving the resistance of a material to fatigue crack propagation. If one's primary objective is to collect data for designs and safety inspections, one can fit the data well to an empirical equation, which contains enough parameters; then use the equation to achieve its engineering objectives. The specific form of the equation and the specific physical model for fatigue crack propagation are not important. On the other hand, if the main objectives are to evaluate and to improve materials, the physical model and the form of an equation become important.

The data in region I and region II are more meaningful for the evaluation of the resistance of a material to fatigue crack propagation. The data in region III is complicated by crack tip necking. In the necking region, the effects of the material properties are mixed with the complicated plastic deformation pattern at a crack tip. In conclusion, one should use a thick specimen for material evaluation so that plane strain case is insured.

If the deformation and fracture properties of a material can be considered homogeneous, if the condition of plane strain is satisfied, and if, $r_e >> r_p$, we have

$$da/dN = f_6 (R)\ \Delta K^2 \qquad (8b)$$

This relation is valid for both shear and/or normal separation mode. It should be emphasized that this relation is not the general law of fatigue crack propagation. But if the above mentioned conditions are all satisfied, this relation has to be correct. Any experimental data that deviates from this relation must be caused by the fact that one or more of these conditions are not complied with. Therefore this analysis helps one to analyze and to evaluate experimental data.

For a particular physical model of fatigue crack propagation, based on either shear or normal separation mode, if one uses a two-dimensional model to analyze fatigue crack propagation in the low $\Delta K$ region, and if one assumes material homogeneity, the mere fact that the data show a relation of the type of Equation (8b) does not offer any verification of the specific model. For example Lehr and Liu (4) have proposed a mechanical model of fatigue crack propagation. They assumed that a material element ahead of a crack tip is damaged by cyclic plastic strain. They used Manson-Coffin's strain controlled fatigue law and Miner's cumulative damage law to derive an equation for fatigue crack propagation.

$$da/dN = C_4\ [\Delta K/\sigma_{Y(c)}]^2\ [\varepsilon_{Y(c)}/M]^2 \qquad (14)$$

where $C_4$ is a constant, $\sigma_{Y(c)}$ and $\varepsilon_{Y(c)}$ are cyclic yield stress and cyclic yield strain and M is the strain range at a cyclic fatigue life of one cycle for a smooth specimen. In the derivation, a two-dimensional model was used and material homogeneity and the condition that $r_e >> r_p$ were assumed. Therefore the mere fact that the data is proportional to $\Delta K^2$ does not verify the proposed cumulative damage model. The model can be verified only if all the material constants, $\Delta K$, and $da/dN$ agree with the equation.

It should be recognized that the analysis is based on an elasto-plastic model. This analysis does not take rate sensitive materials into consideration nor any crack growth mechanisms that are rate sensitive. The analyses on crack growths in viscoelastic materials and the diffusion controlled and chemical reaction rate controlled crack growth mechanisms have yet to be done.

## VIII. CONCLUSIONS

1. At a constant value of R, da/dN is proportional to "a" if a plate is large and thick, if the average deformation and fracture properties over the crack increment, $\Delta a$, are homogeneous, and if the characteristic discrete lengths of the deformation and fracture processes are smaller than the crack increment per cycle, $\delta a$. The last two conditions are referred to as the conditions of "material homogeneity". The condition $r_e >> r_p$ is not necessary.

2. da/dN is a function of $\Delta K$ and R, if a plate is thick enough so that plane strain condition prevails and if the applied stress is low in comparison with the yield strength. The conditions of "material homogeneity" are not necessary.

3. da/dN is proportional to $\Delta K^2$ at a given value of R, if a plate is thick enough, if the applied stress is low in comparison with the yield strength, and if the conditions of homogeneity are satisfied.

## APPENDIX: DIMENSIONAL ANALYSIS ON THE ELASTO-PLASTIC STRESSES AND STRAINS AT HOMOLOGOUS POINTS OF GEOMETRICALLY SIMILAR SOLIDS AND CRACKED PLATES

The $\pi$ theorem is often used to make dimensional analysis (42) According to this theorem, several independent dimensionless parameters are formed to correlate experimental data. A correct choice of a set of dimensionless parameters gives a meaningful empirical correlation. On the other hand, a wrong choice of the parameters may lead to erroneous conclusions. This difficulty can be avoided if the basic physical laws of a problem are known and can be written in mathematical equations. These equations help to choose a set of meaningful dimensionless parameters. In this study, the geometrically similar solids made of the same material will be analyzed. For such solids, their geometric shapes are the same. The only difference is in their sizes. The size of such a solid can be specified by a characteristic length, L. The set of equations that govern the stresses and strains in these solids can be written as follows:

$$\frac{\partial \sigma_{ij}}{\partial X_i} = 0 \tag{A1}$$

$$\varepsilon_{ij,k\ell} + \varepsilon_{k\ell,ij} - \varepsilon_{ik,j\ell} - \varepsilon_{j\ell,ik} = 0 \tag{A2}$$

$$\varepsilon_{ij} = \frac{1}{2}\left[\frac{\partial U_i}{\partial X_j} + \frac{\partial U_j}{\partial X_i} - \frac{\partial U_k}{\partial X_i}\frac{\partial U_k}{\partial X_j}\right] \tag{A3}$$

$$de_{ij} = \frac{3S'_{ij}\, d\,\sigma_{eff}}{2\sigma_{eff}\, H'} + \frac{dS_{ij}}{2G} \tag{A4}$$

$$d\varepsilon_{ii} = \frac{(1-2\nu)}{E}\, d\,\sigma_{ii} \tag{A5}$$

where $\sigma_{ij}$ and $\varepsilon_{ij}$ are stress and strain tensors; $S_{ij}$ and $e_{ij}$ are deviatoric stress and strain tensors; $\sigma_{eff}$ is effective stress; H' is the slope of the effective stress plastic strain curve; E, G, and $\nu$ are Young's modulus, shear modulus and Poisson's ratio respectively; and $U_i$ and $X_i$ are dimensionless displacement vector and the coordinates which are defined as

$$U_i = \frac{u_i}{L} \tag{A6}$$

and

$$X_i = \frac{x_i}{L} \tag{A7}$$

$u_i$ and $x_i$ are displacement vector and the coordinate system. The summation convention of index notation is used; and the comma between indices denotes differentiation. For detailed discussions on the index notation, readers are referred to Reference (43). If the geometrically similar solids are scaled by their respective L's, the geometry of the solids in the $X_i$ space are identical. These equations indicate clearly that with the same applied stresses on the boundaries, specified in terms of $X_i$, the stresses and strains at homologous points, $X_i$, i.e. at geometrically similar points, must be identical.

The above conclusion is valid for geometrically similar elasto-plastic solids under the same stress boundary conditions at geometrically similar points on the boundaries. A concentrated force $F_i$ on a boundary can be treated as a very high stress $\overset{\nu}{T}_i$ acting on a small area $\Delta A$. That is

$$F_i = \lim_{\Delta A \to 0} \overset{\nu}{T}_i \, \Delta A \tag{A8}$$

For a concentrated line force acting on the boundary of a plate, the condition of identical boundary stress at the geometrically similar points requires that the force is linearly proportional to the size of the plate, in order to have identical stresses and strains at homologous points in geometrically similar solids.

The preceding condition imposed on the line force of two-dimensional problems can be illustrated by the elastic calculation of the stresses in the vicinity of a crack tip in a centrally cracked infinite plate with two

opposite wedge forces acting at the mid-points of the cracked surfaces as shown schematically in Figure (2).

$$F = \lim_{\Delta A \to 0} \sigma \Delta A$$

$$= \lim_{\Delta W \to 0} \sigma t \, \Delta W \qquad (A9)$$

where W is the width of the narrow strip of the area on which the concentrated force is acting and t is the thickness of the plate. The stresses in the vicinity of the crack tip are proportional to the applied stress, $\sigma$, and the characteristic crack tip stress singularity, $\sqrt{a/2\pi r}$. Therefore the stresses in the vicinity of the crack point can be written as

$$\sigma_{ij} = C_5 \, \sigma \sqrt{\frac{a}{2\pi r}} \, f_{ij}(\theta) \qquad (A10)$$

Substituting (A9) into (A10), one obtains

$$\sigma_{ij} = C_6 \frac{F}{\Delta W} \sqrt{\frac{a}{2\pi r}} \, f_{ij}(\theta) \qquad (A11)$$

where $C_5$ and $C_6$ are constants. The condition of similarity requires that $\Delta W$ is proportional to the crack gength, a. Hence

$$\sigma_{ij} = C_3 \frac{F}{\sqrt{2\pi r a}} \, g_{ij}(\theta) \qquad (A12)$$

where $C_3$ is a proportional constant. The elastic calculation indicates that

$$\sigma_{ij} = \frac{F}{\pi \sqrt{2ra}} \, g_{ij}(\theta) \qquad (A13)$$

The constant $C_3$ in Equation (A12) is equal to $\sqrt{1/\pi}$. It should be noticed that the above discussion on the stress intensity factor is for an elastic cracked plate. Our earlier conclusion for geometrically similar solids is valid for general elasto-plastic solids. The elastic example is only a special case.

The above conclusions are valid for problems which have only one characteristic length. For problems involving more than one quantity with linear dimension, such as thickness, grain size, lattice spacing etc., the above deductions are no longer valid.

REFERENCES


1. A. K. Head, "On the Growth of Fatigue Cracks," The Philosophical Magazine, Vol. 44, Series 7c, 1953, p. 725.

2. N. E. Frost and D. S. Dugdale, "The Propagation of Fatigue Cracks in Sheet Specimens," Journal of the Mechanics and Physics of Solids, Vol. 6, No. 2, 1958, p. 92-110.

3. H. W. Liu, "Crack Propagation in Thin Metal Sheets Under Repeated Loading," The Journal of Basic Engineering, Trans. ASME Vol. 83, Series D, No. 1, March 1961, p. 23-31.

4. Kenneth R. Lehr and H. W. Liu, "Fatigue Crack Propagation and Strain Cycling Properties," International Journal of Fracture Mechanics, Vol. 5, No. 1, March 1969.

5. H. W. Liu and N. Iino, "A Mechanical Model for Fatigue Crack Propagation," Fracture: Proceedings of the Second International Conference on Fracture, Brighton, April 1969.

6. P. C. Paris, M. P. Gomez and W. E. Anderson, "A Rational Analytic Theory of Fatigue," The Trend in Engineering, Vol. 13, January 1961, p. 9.

7. P. C. Paris and F. Erdogan, "A Critical Analysis of Crack Propagation Laws," An ASME publication, Paper No. 62-WA-234.

8. P. C. Paris, "The Fracture Mechanics Approach to Fatigue," Tenth Sagamore Materials Research Conference, Fatigue - An Interdisciplinary Approach, Syracuse University Press, 1964.

9. F. A. McClintock, "On the Plasticity of the Growth of Fatigue Cracks," Fracture of Solids, John Wiley, New York, 1963, p. 65.

10. J. Schijve, "Significance of Fatigue Cracks in Micro-Range and Macro-Range," Fatigue Crack Propagation, STP 415 American Society for Testing and Materials, 1967.

11. W. G. Clark, Jr. and H. E. Trout, Jr., "Influence of Temperature and Section Size on Fatigue Crack Growth Behavior in Ni-Mo-V Alloy Steel," Engineering Fracture Mechanics, Vol. 2, No. 2, Nov. 1970.

12. R. J. Donahue, H. McI. Clark, P. Atanmo, R. Kumble, and A. J. McEvily, "Crack Opening Displacement and the Rate of Fatigue Crack Growth," Report, Institute of Materials Science, The Univ. of Connecticut, 1971.

13. J. M. Krafft, "On Prediction of Fatigue Crack Propagation Rate from Fracture Toughness and Plastic Flow Properties," A.M.S. Trans. 58, 1965, p.691.

14. J. R. Rice, "Mechanics of Crack Tip Deformation and Extension by Fatigue," Fatigue Crack Propagation ASTM. STP 415, 1967, p. 247.

15. Cambell Laird, "The Influence of Metallurgical Structure on the Mechanisms of Fatigue Crack Propagation," Fatigue Crack Propagation, STP 415 Am. Soc. for Testing and Materials, 1967.

16. B. Tomkins, "Fatigue Crack Propagation - An Analysis," Phil. Mag., Vol. 18, Nov. 1968, No. 155, p. 1041-1066.

17. Maria Roney, "Fatigue of High-Strength Materials," Fracture, An Advanced Treatise, Edited by H. Liebowitz, Vol. III, Academic Press, 1971.

18. Herbert H. Johnson and P. Paris, "Sub-Critical Flaw Growth," Engineering Fracture Mechanics, Vol. 1, No. 1, June 1968.

19. M. L. Williams, "On the Stress Distribution at the Base of a Stationary Crack," Jour. of Applied Mech., March 1957, p. 109-114.

20. G. R. Irwin, "Annalysis of Streses and Strains Near the End of a Crack Traversing a Plate," Jour. of Appl. Mech., Sept. 1957, p. 361-364.

21. T. S. Kang and H. W. Liu, "Cyclic Deformation at a Crack Tip," Syracuse University Report, Jan. 1972.

22. John M. Barsom, "Investigation of Sub-critical Crack Growth," Doctoral Dissertation, University of Pittsburgh, 1969.

23. D. S. Dugdale, "Yielding of Steel Sheets Containing Slits," J. Mech. and Physics of Solids, Vol. 8, 1960, p. 100.

24. J. N. Goodier and F. A. Field, "Plastic Energy Dissipation in Crack Propagation," Fracture of Solids, John Wiley, New York, 1963, p. 103.

25. B. A. Bibly, A. H. Cottrell and K. H. Swinden, "The Spread of Plastic Yield From a Notch," Proc. Roy. Soc., London, A272, 1963, p. 304.

26. J. R. Rice, "Plastic Yielding at a Crack Tip," The First International Conference on Fracture, Sendai, Japan, 1965, p. 283.

27. B. J. Schaeffer, H. W. Liu and J. S. Ke., "Deformation and the Strip Necking Zone in a Cracked Steel Sheet," Experimental Mechanics, April 1971.

28. R. D. Heidenreich and W. Shockley, "Report on Strength of Solids," Physical Society, London, 1948.

29. H. G. van Bueren, "Imperfections in Crystals," Second Edition, North Holland Publishing Co., 1961, p. 135.

30. J. R. Hancock and J. C. Grosskreutz, "Mechanisms of Fatigue Hardening in Copper Single Crystal," Acta Met., Vol. 17, 1969 p. 77.

31. R. J. Stokes and C. H. Li, "The Anisotropic Extension of Micro-cracks by Plastic Flow in Semi-Brittle Solids," Fracture of Solids, John Wiley and Sons, 1963.

32. Earl R. Parker, "Fracture of Ceramic Materials, " Fracture, John Wiley and Sons, Inc., 1959, p. 181.

33. J. J. Gilman, A Discussion on "Theoretical Aspects of Fracture," by A. H. Cottrell, Fracture, John Wiley and Sons, Inc., 1959, p. 52.

34. J. D. Eshelby, F. C. Frank and F. R. N. Nabarro, "The Equilibrium of Linear Arrays of Dislocations," Phil. Mag., Vol. 42, 1951, p. 351.

35. H. W. Liu, "Shear Cracks and Double-Ended Dislocation Array," J. of Applied Physics, Vol. 36, No. 4, April 1965, p. 1468-1470.

36. A. N. Stroh, "A Theory of the Fracture of Metals," Advances in Physics, Vol. 6, 1957, p. 418.

37. G. T. Hahn, B. L. Averbach, W. S. Owen and Morris Cohen, "Initiation of Cleavage Micro-cracks in Polycrystalline Iron and Steel," Fracture, John Wiley and Sons, 1959, p. 91.

38. D. A. Ryder and A. C. Smale, "A Metallographic Study of Tensile Fractures in Aluminum - Copper and Aluminum - Copper - Zinc - Magnesium Alloys," Fracture in Solids, John Wiley and Sons, 1963.

39. W. A. Wood, S. McK. Couslaud and K. R. Sargaut, "Systematic Microstructural Changes Peculiar to Fatigue Deformation," Acta. Met., Vol. 2, No. 7, July 1963.

40. P. J. E. Forsyth, "Fatigue Damage and Crack Growth in Aluminum Alloy," Acta. Met., Vol. 2, No. 7, July 1963.

41. J. C. Grosskrentz and G. G. Shaw, "Critical Mechanisms in the Development of Fatigue Cracks in 2024-T4 Aluminum," Fracture, 1969, P. L. Pratt, Ed., Chapman and Hall, London, 1969, p. 620.

42. Henry Louis Langhaar, "Dimensional Analysis and Theory of Models," John Wiley and Sons, New York, 1951.

43. Y. C. Fung, "Foundations of Solid Mechanics," Prentice Hall, New York, 1965.

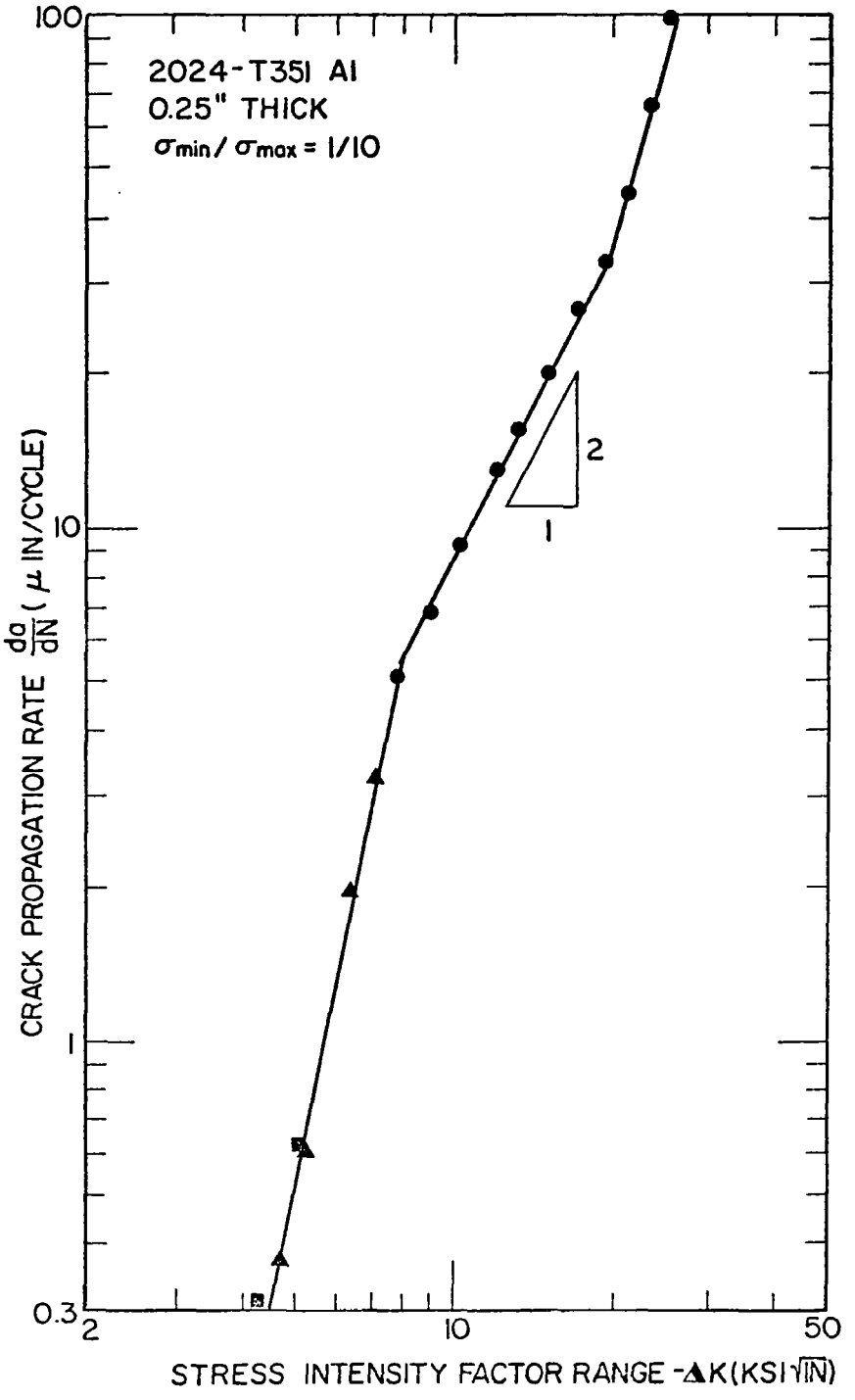


FIGURE (1a) TYPICAL FATIGUE CRACK PROPAGATION DATA FOR 2024-T351 ALUMINUM ALLOY.

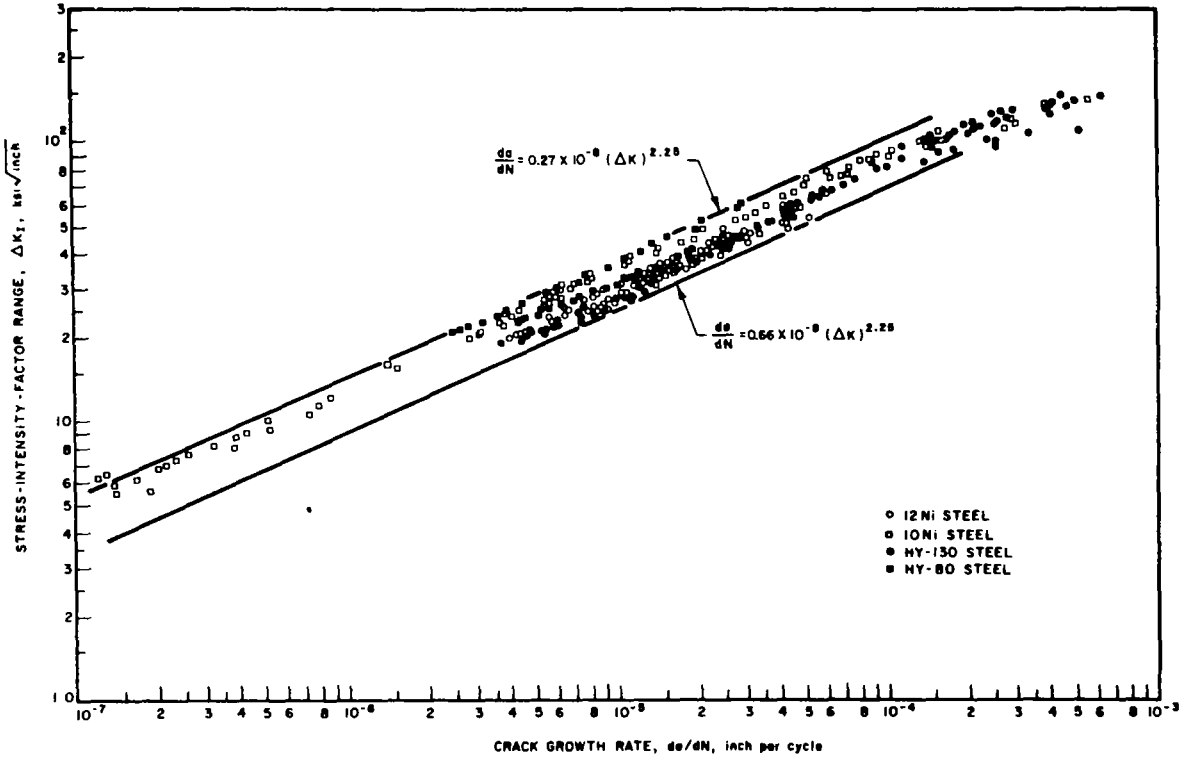


FIGURE (1b) FATIGUE-CRACK-PROPAGATION DATA FOR HIGH STRENGTH STEELS.(Ref.22)

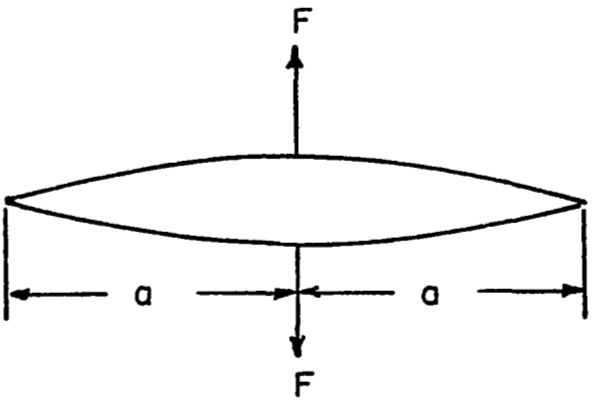


FIGURE (2) A CRACK IN AN INFINITE PLATE WITH TWO WEDGE FORCES.

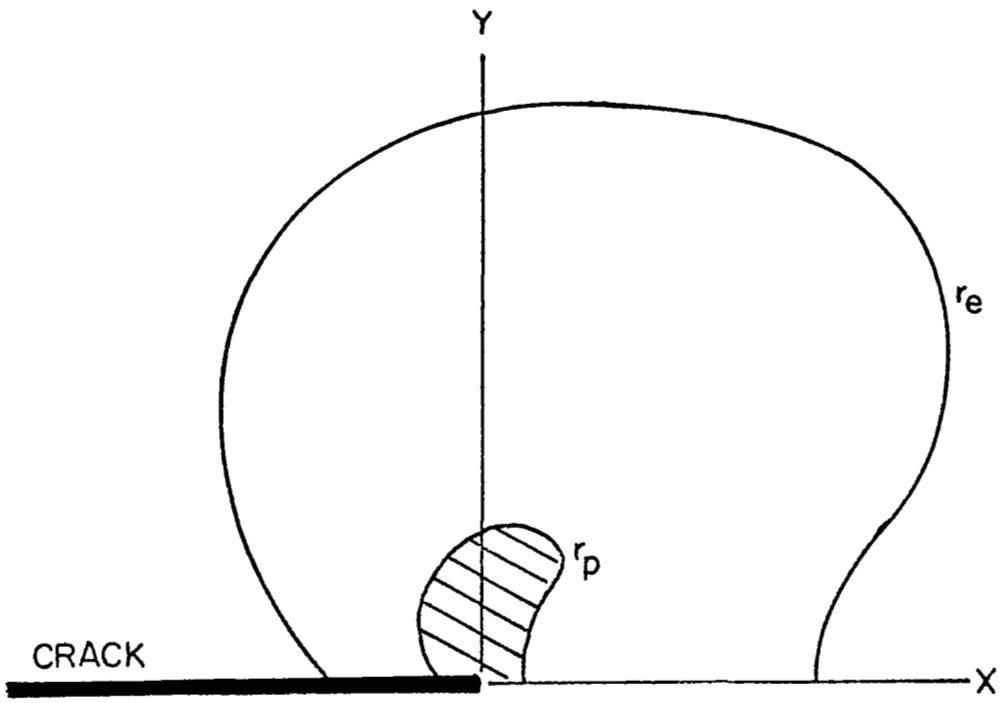


FIGURE (3) SCHEMATIC REPRESENTATION OF $r_e$ AND $r_p$ NEAR A CRACK TIP.

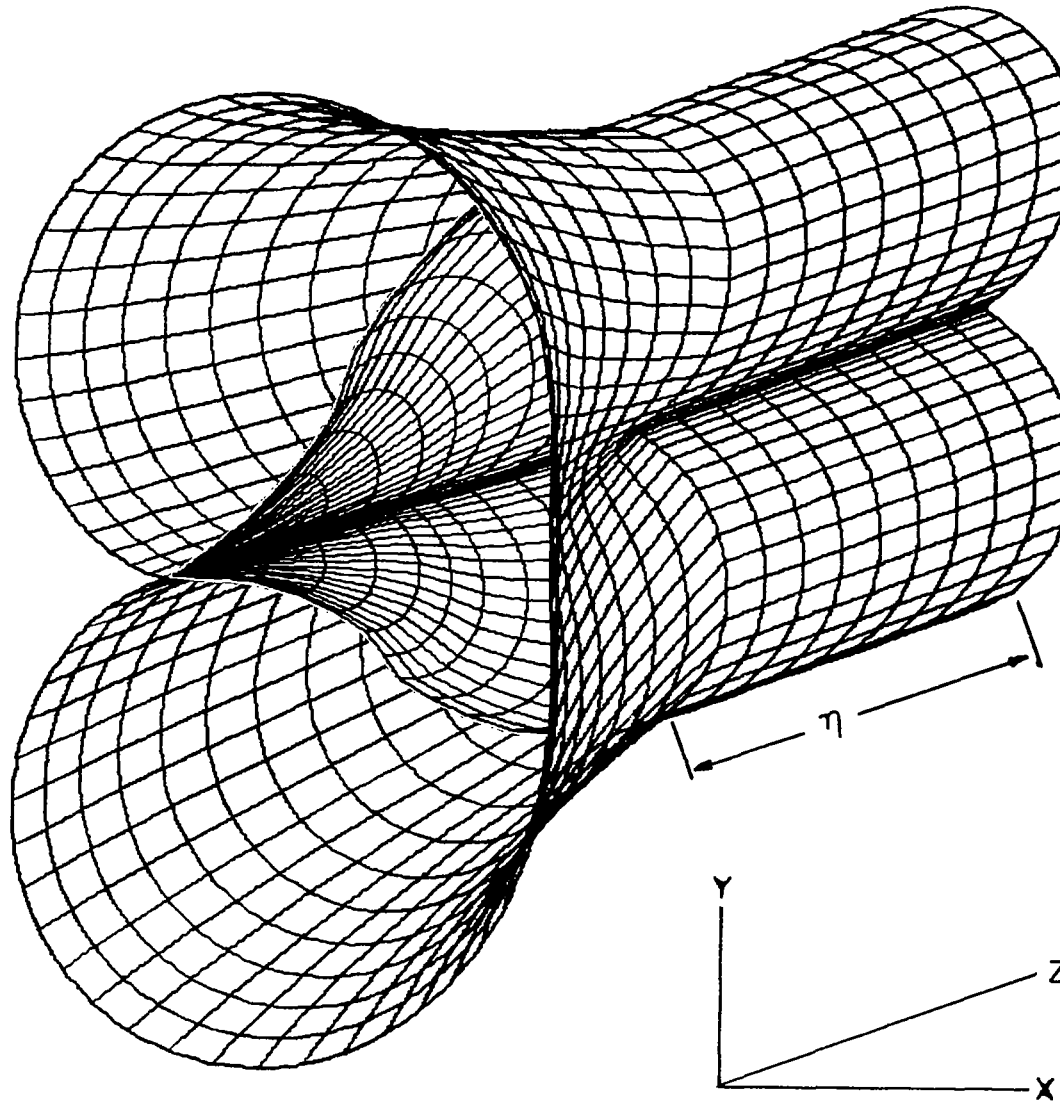


FIGURE (4) SCHEMATIC DIAGRAM SHOWING THE PLASTIC ZONE. ONLY HALF OF THE ZONE IS SHOWN. THE PLANE STRAIN PLASTIC ZONE IS IMBEDDED. (Courtesy Mr. W. L. Hu)

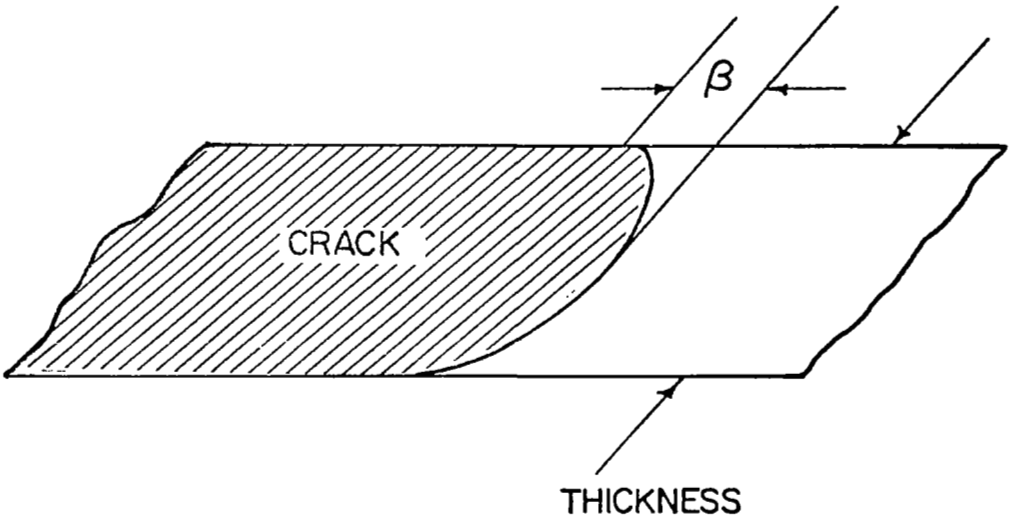


FIGURE (5) A TWO-DIMENSIONAL SCHEMATIC FIGURE OF A CRACK FRONT.

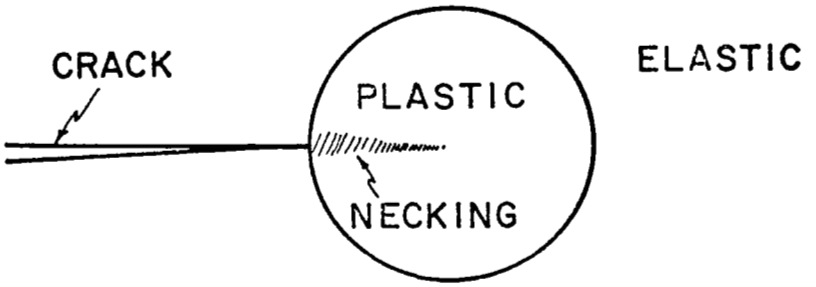


FIGURE (6) A STRIP NECKING ZONE IMBEDDED IN A PLASTIC REGION.

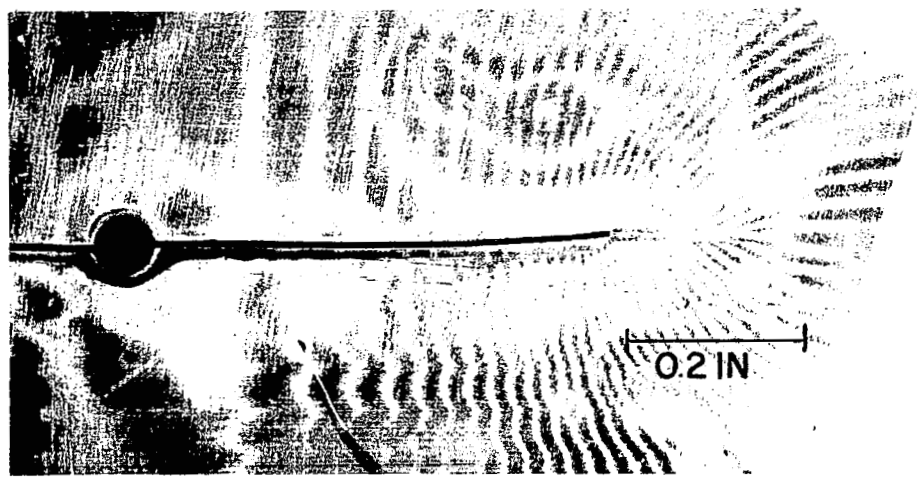


FIGURE (7) MOIRE PATTERN OF A STEEL SPECIMEN: APPLIED STRESS 55 KSI; 0.2% OFFSET YIELD STRESS 91 KSI; YOUNG'S MODULUS $32 \times 10^6$ PSI; 0.012 INCHES THICK; 6 INCHES WIDE; SLOT LENGTH 1 INCH; PITCH OF MOIRE GRILLE 1/13,400 INCHES.

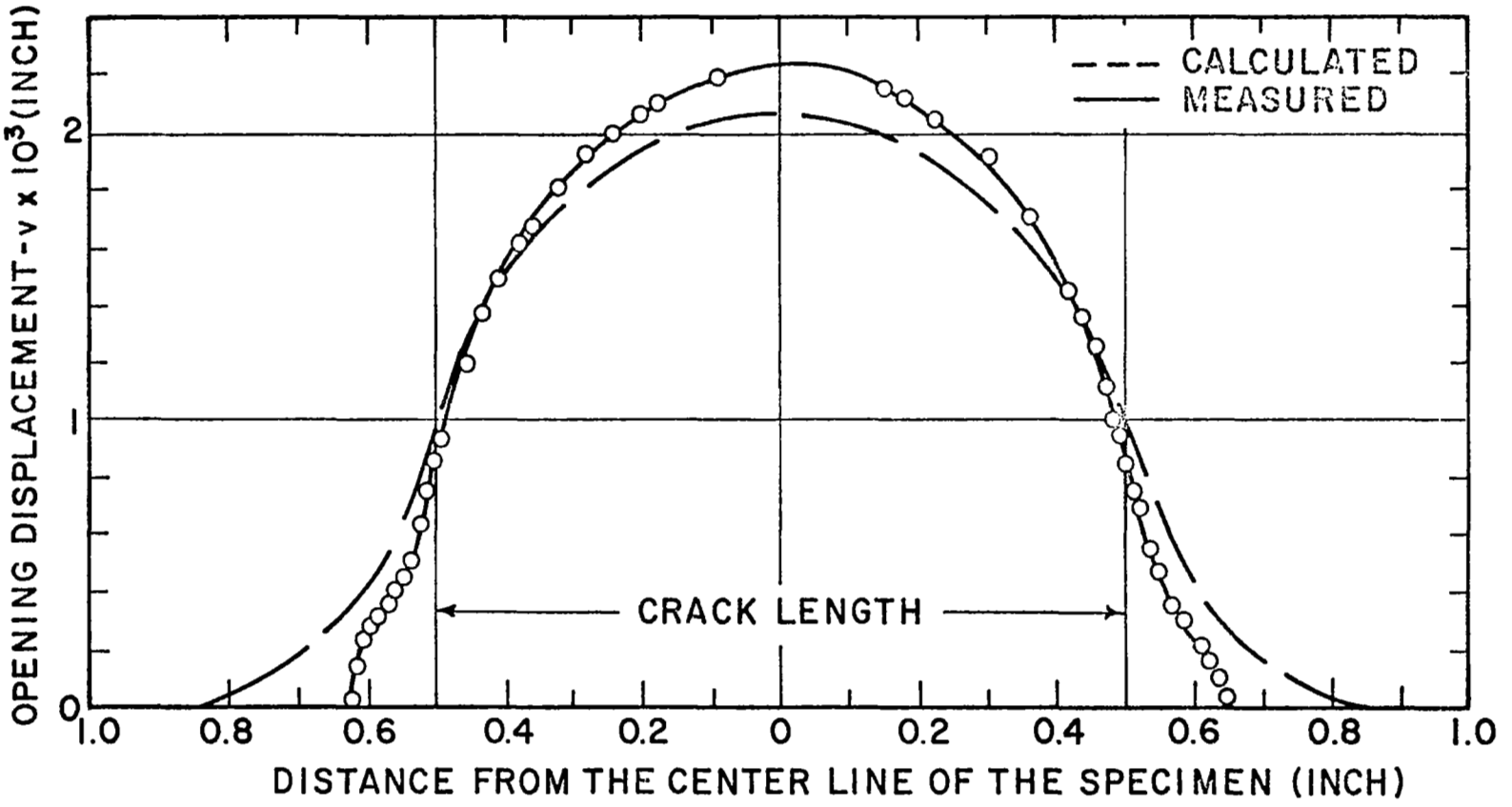


FIGURE (8) OPENING DISPLACEMENT ALONG CRACK LINE: $\sigma$, 55 KSI; $\sigma_Y$, 91 KSI: E, 32 X $10^6$ PSI; THICKNESS, 0.012 INCHES; WIDTH, 6 INCHES; SLOT LENGTH, 1.0 INCH.

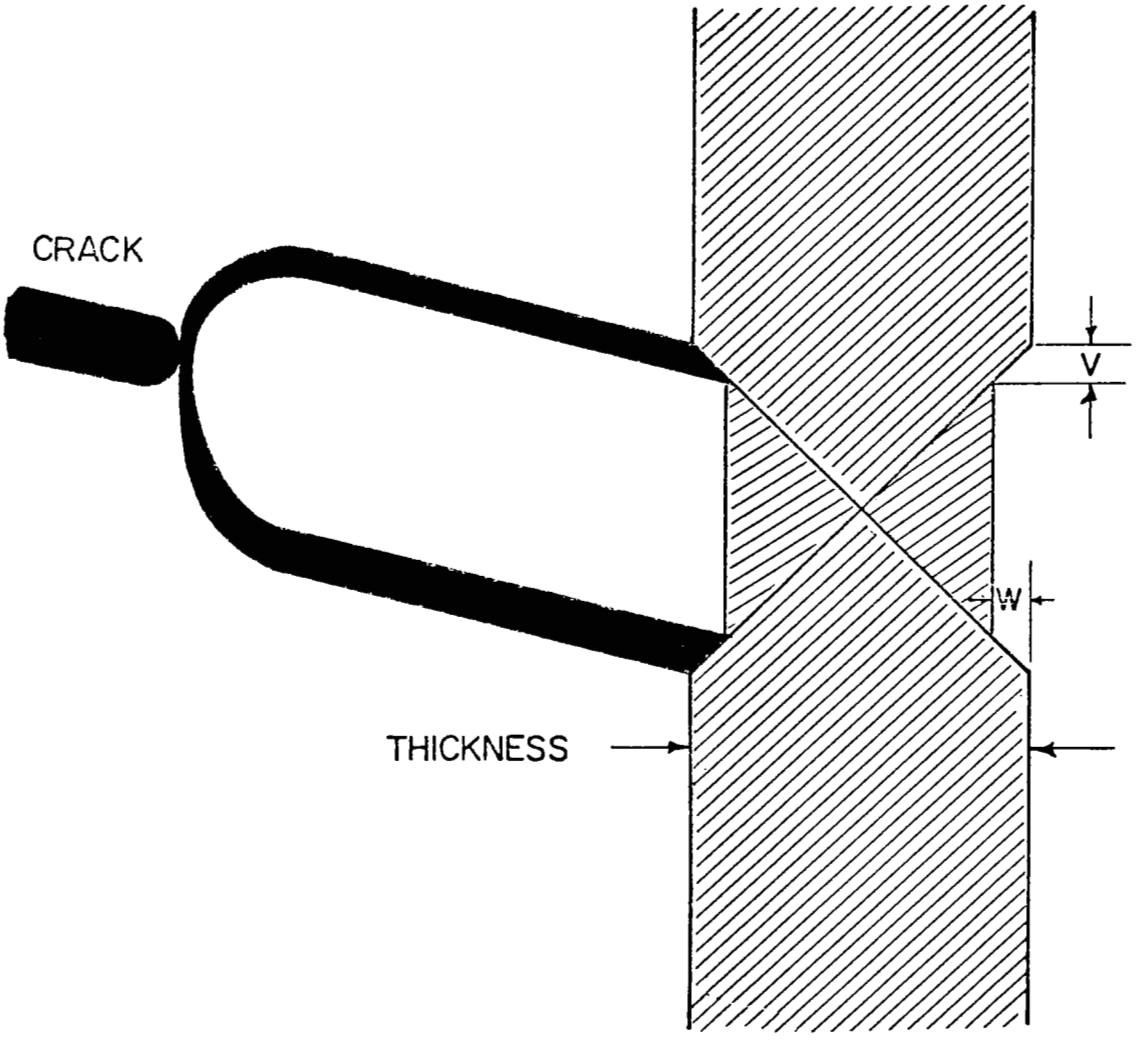


FIGURE (9) SCHEMATIC DIAGRAM FOR NECKING ZONE AHEAD OF A CRACK.

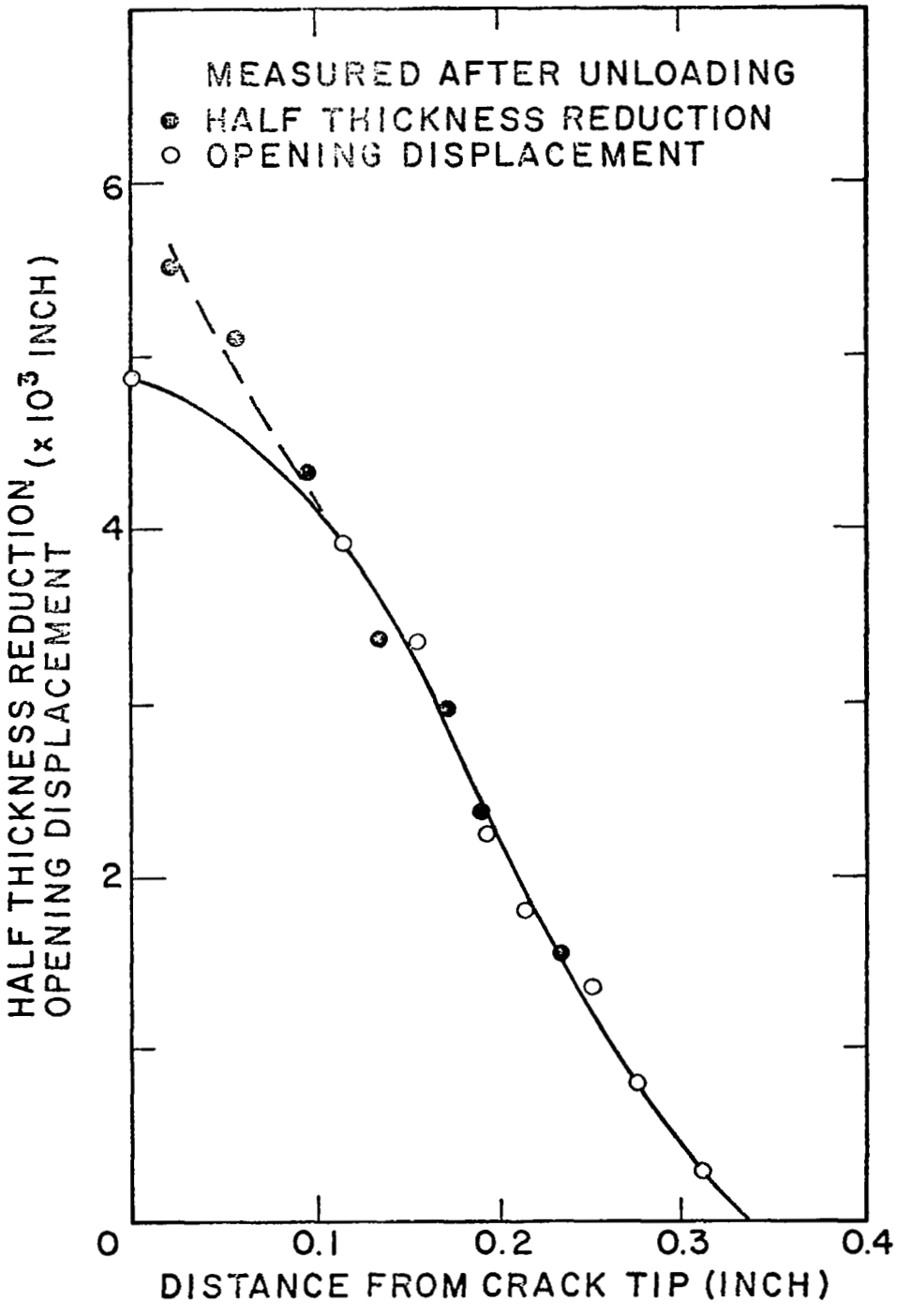


FIGURE (10) HALF OF THICKNESS REDUCTION AND OPENING DISPLACEMENT IN THE NECKING REGION OF A STEEL SHEET: $\sigma$ 62 KSI; $\sigma_Y$, 91 KSI; E, 32 X $10^6$ PSI: THICKNESS 0.012 INCHES: WIDTH, 6 INCHES; SLOT LENGTH 1.0 INCH.

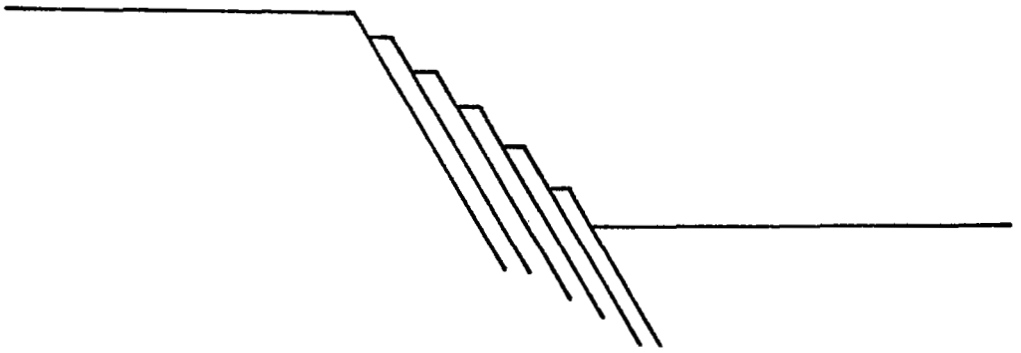

FIGURE (11) A GLIDE LAMELLA.

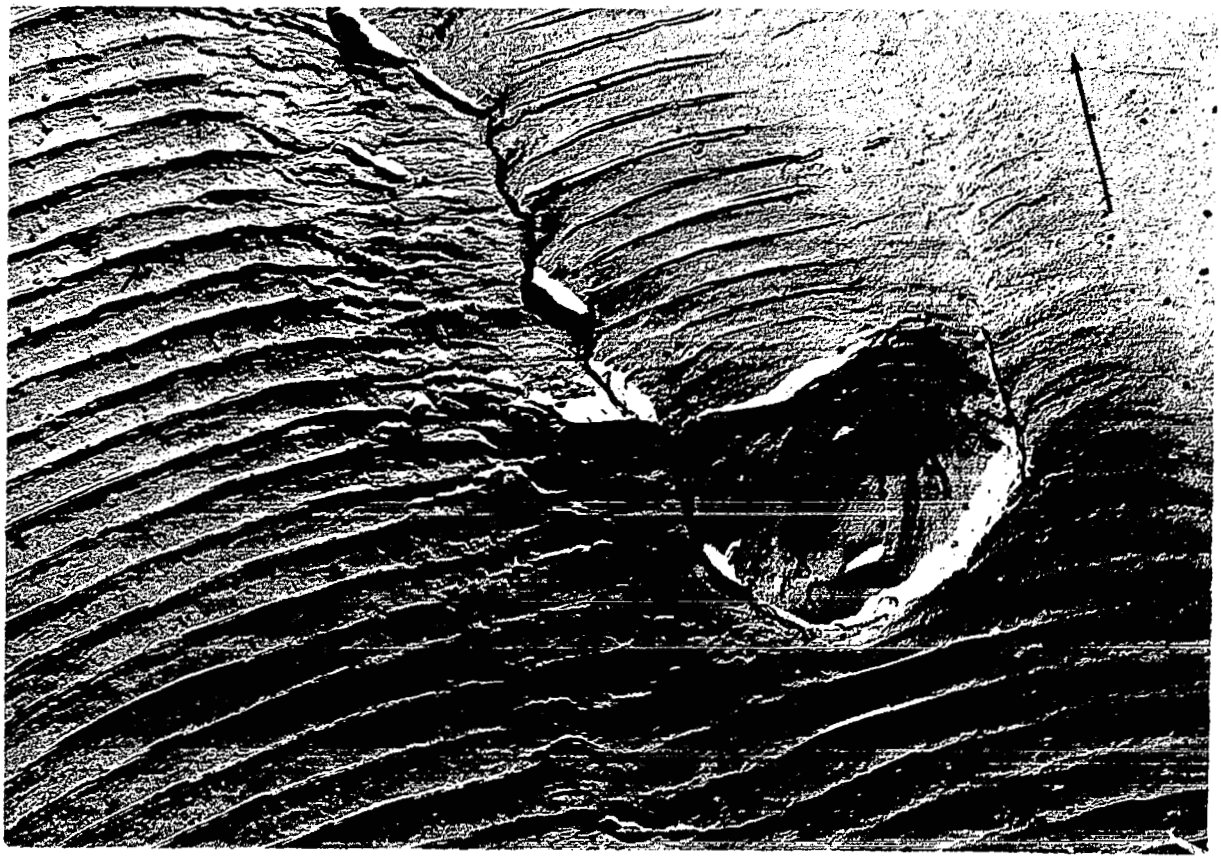

FIGURE (12) CLEAVAGE FRACTURE, SHEAR STEPS AND STRIATIONS.

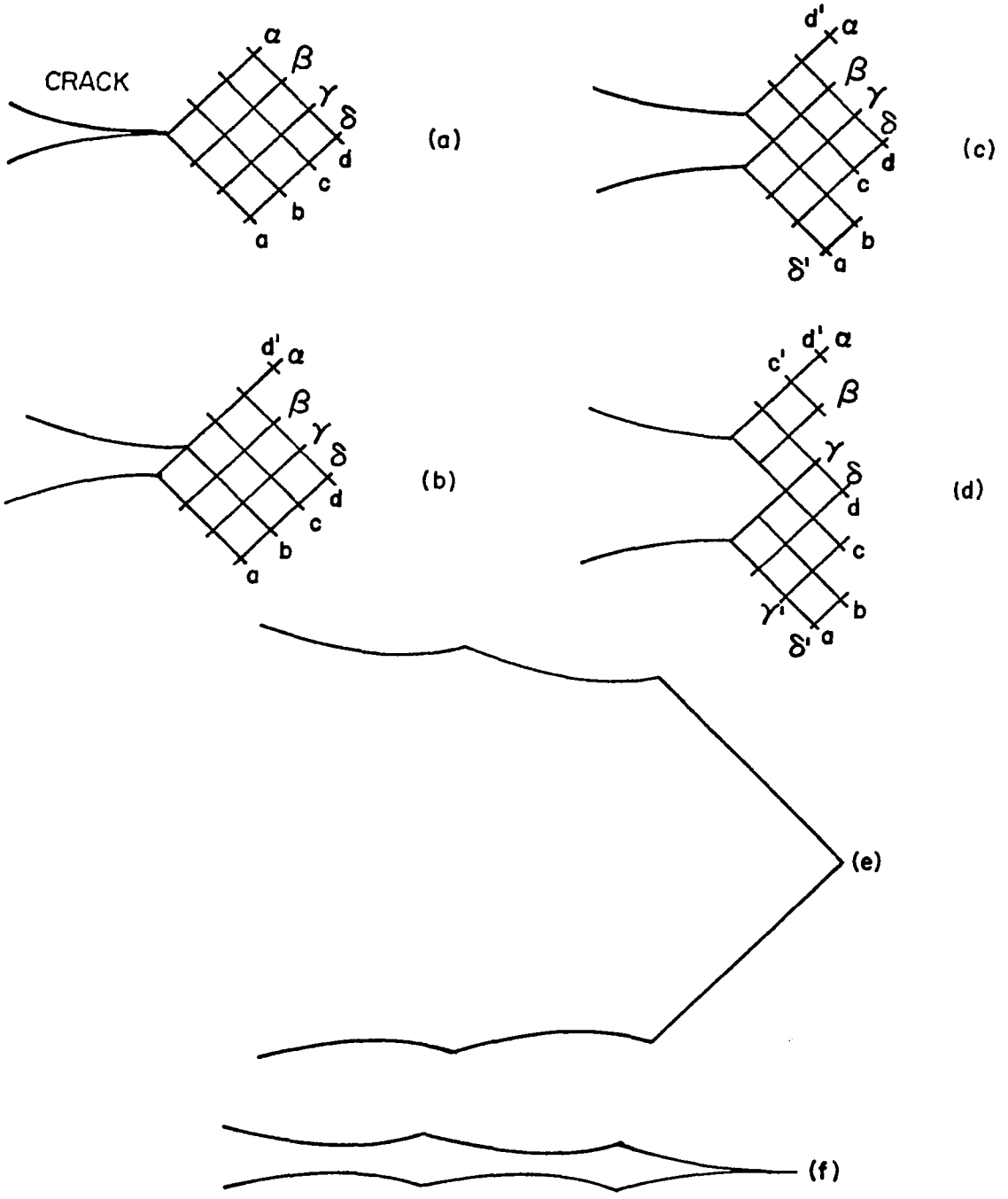


FIGURE (13) SUCCESSIVE DISCRETE SHEAR SEPARATIONS CAUSE CRACK TIP OPENING. (a), (b), (c), (d) SHEAR SEPARATION MOVEMENTS ALONG SLIP LINES DURING THE LOADING CYCLE. (e) CRACK OPENING AT MAXIMUM LOAD. (f) CRACK PROFILE UPON UNLOADING.

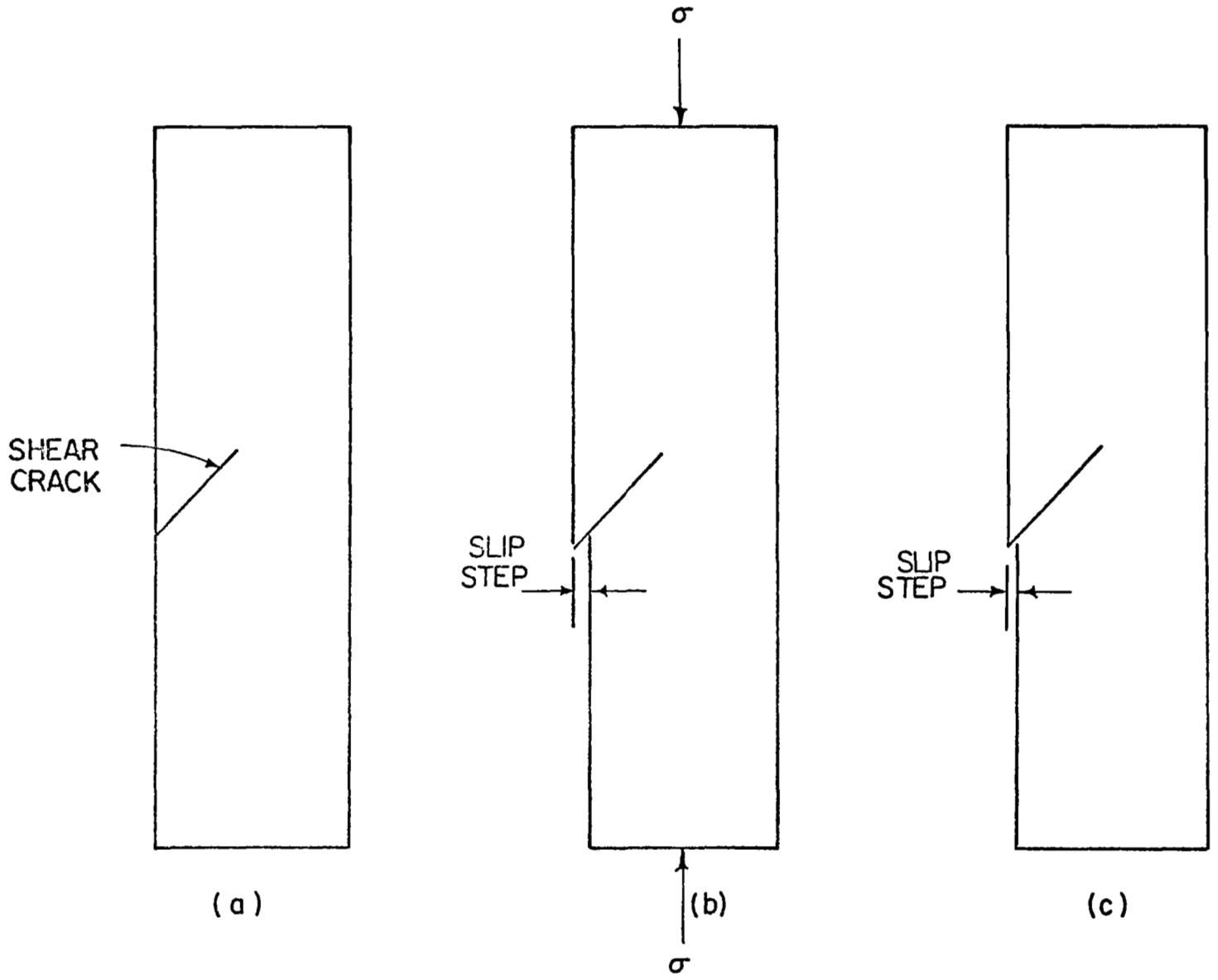


FIGURE (14) THE SLIP STEP OF A SHEAR CRACK UNDER COMPRESSION WITH FRICTIONAL SHEAR STRESS BETWEEN CRACK SURFACES (a) BEFORE LOADING (b) AT MAXIMUM COMPRESSION (c) UPON UNLOADING.